

***In vitro* roles of invariant helix–turn–helix motif residue R383 in σ^{54} (σ^N)**

Siva R. Wigneshweraraj, Akira Ishihama¹ and Martin Buck*

Department of Biology, Imperial College of Science, Technology and Medicine, Sir Alexander Fleming Building, Imperial College Road, London SW7 2AZ, UK and ¹Department of Molecular Genetics, National Institute of Genetics, Mishima, Shizuoka 411, Japan

Received October 24, 2000; Revised and Accepted December 13, 2000

ABSTRACT

***In vitro* DNA-binding and transcription properties of σ^{54} proteins with the invariant Arg383 in the putative helix–turn–helix motif of the DNA-binding domain substituted by lysine or alanine are described. We show that R383 contributes to maintaining stable holoenzyme–promoter complexes in which limited DNA opening downstream of the –12 GC element has occurred. Unlike wild-type σ^{54} , holoenzymes assembled with the R383A or R383K mutants could not form activator-independent, heparin-stable complexes on heteroduplex *Sinorhizobium meliloti nifH* DNA mismatched next to the GC. Using longer sequences of heteroduplex DNA, heparin-stable complexes formed with the R383K and, to a lesser extent, R383A mutant holoenzymes, but only when the activator and a hydrolysable nucleotide was added and the DNA was opened to include the –1 site. Although R383 appears inessential for polymerase isomerisation, it makes a significant contribution to maintaining the holoenzyme in a stable complex when melting is initiating next to the GC element. Strikingly, Cys383-tethered FeBABA footprinting of promoter DNA strongly suggests that R383 is not proximal to promoter DNA in the closed complex. This indicates that R383 is not part of the regulatory centre in the σ^{54} holoenzyme, which includes the –12 promoter region elements. R383 contributes to several properties, including core RNA polymerase binding and to the *in vivo* stability of σ^{54} .**

INTRODUCTION

The promoter specificity of bacterial RNA polymerases (RNAP) is determined by the σ subunit present in the holoenzyme ($E\sigma$). Two classes of σ factors, σ^{70} and σ^{54} (σ^N), have been identified. In marked contrast to the σ^{70} factor, σ^{54} associates with core RNAP to form a holoenzyme that binds to promoter DNA forming a closed complex that rarely spontaneously isomerises to the open complex. Conversion of the σ^{54} holoenzyme closed complex to a transcription-competent open

complex is dependent upon γ – β bond hydrolysis of nucleoside triphosphates by activator proteins that bind DNA elements with enhancer-like properties. Activation is mediated by direct activator–closed complex interactions (1–6).

Promoter-specific DNA-binding activity of σ^{54} is central to formation of the $E\sigma^{54}$ –promoter complex. DNA binding by σ^{54} appears complex and the interaction between σ^{54} and DNA is modulated by core RNAP (7,8). The promoter sequence recognised by $E\sigma^{54}$ is generally characterised by the presence of GG and GC doublets 24 and 12 bp, respectively, upstream of the transcription initiation point (9). The specific DNA-binding determinants of σ^{54} are located in the C-terminal Region III (residues 329–477 in *Klebsiella pneumoniae*). Included are a putative helix–turn–helix (HTH) motif (residues 367–386) and a patch (residues 329–346) that UV cross-links to DNA, each located C-terminal to the core RNAP-binding domain (residues 120–215) (10–15).

The N-terminal Region I has important regulatory roles in $E\sigma^{54}$ function, including effects on DNA binding (8,16,17). Region I sequences also bind to core RNAP, an interaction suggested to control properties of the holoenzyme important for activator responsiveness, but dispensable for core RNAP binding *per se* (7,10,13,18,19). The solvent accessibility of sequences within the DNA-binding domain of σ^{54} is changed in the holoenzyme when Region I is deleted, suggesting that Region I contributes to physical properties of the holoenzyme, some of which involve sequences that are closely associated with the DNA-binding function of σ^{54} (7). Holoenzymes formed with mutant or deleted Region I σ^{54} function in activator-independent transcription, in which the promoter-bound $E\sigma^{54}$ isomerises and produces transcripts via an unstable open promoter complex (17,20,21–24). Mutant or deleted Region I σ^{54} proteins display changes in DNA-binding activity associated with recognition of the local DNA melting that occurs next to the consensus GC element upon closed complex formation (8,25,26). Proper recognition of this local DNA melting downstream to the GC is a hallmark for regulated transcription initiation by $E\sigma^{54}$ (8,10,15,26). The GC promoter region of σ^{54} -dependent promoters is known to be a key DNA element contributing to the network of interactions that keep the polymerase in the closed complex and limit DNA opening prior to activation (8,22,27). Region I, the σ^{54} UV cross-linking patch and the –12 promoter region form a centre in the

*To whom correspondence should be addressed. Tel: +44 20 7594 5442; Fax: +44 20 7594 5419; Email: m.buck@ic.ac.uk

holoenzyme that contains protein and DNA determinants for activator responsiveness and DNA melting (15,17,22,27,28).

Region III residues 367–386 of σ^{54} are proposed to form a HTH DNA-binding structure. R383 in the recognition helix is suggested to interact with bases in the –12 promoter element, in particular with the consensus G of the GC promoter doublet (14). Substitution of R383 with any other amino acid except lysine and, to a lesser extent, histidine was suggested to result in an inactive protein, implying that the nature of the charge on this residue is important for σ^{54} function (14). The suppression of –12 promoter-down mutations in the *K.pneumoniae glnAp2* promoter by R383K *in vivo* is considered as evidence for a role for R383 in recognition of the –12 promoter region. An extension of these conclusions was that the promoter interaction was direct, based largely on the idea that the suggested bi-helical structure would make specific contacts to promoter DNA and that the apparent suppression data might not be explained by indirect effects (14).

Here we have explored the functionality of purified σ^{54} proteins altered at position 383 to determine if R383 is part of the regulatory centre in the σ^{54} holoenzyme. Results indicate that R383 is not a part of the centre and that R383 may not establish a direct contact to DNA. Rather it seems that residue 346 is part of the centre and is close to the GC promoter region. However, it is clear that R383 contributes to DNA binding and discrimination between bases at the G of the GC. It is also required for σ^{54} stability *in vivo*. We show that R383 contributes to maintaining stable promoter complexes in which limited one base DNA opening downstream of the –12 GC element has occurred. Although R383 appears inessential for polymerase isomerisation, it appears to make a significant contribution to maintaining the holoenzyme in a stable complex when melting is initiating next to the GC element.

MATERIALS AND METHODS

Site-directed mutagenesis

Plasmids pSRW-R383K and pSRW-R383A expressing *K.pneumoniae* σ^{54} as an N-terminal His₆-tagged protein with alanine or lysine substitution, respectively, at residue R383 were created using the Quickchange mutagenesis kit (Stratagene) as previously described (18). Briefly, pET28::rpoN (pMTH σ^N) plasmid DNA (29) was used as template with a large molar excess of complementary mutagenic primers. Following mutagenesis PCR, DNA was transformed into *Escherichia coli* strain XL2B and mutant clones were identified by sequencing. The BamHI–HindIII fragment carrying part of the C-terminal Region III of σ^{54} and harbouring the R383 mutations was cloned into pMT1/306 (29). A cysteine-free σ^{54} [pSRW-Cys(–)] was created by changing the native cysteines at positions 198 and 346 by site-directed mutagenesis using pMTH σ^N as template. pSRW-Cys(–) was used to introduce a cysteine at position R383 to generate pSRW-R383C (18).

Immunoblotting

Mutant plasmids pSRW-R383K and pSRW-R383C were transformed into *E.coli* strain TH1 ($\Delta rpoN2518$, *endA1*, *thi1*, *hdsR17*, *supE44*, $\Delta lacU169$), which has a deletion of chromosomal *rpoN*, and grown in Luria Broth (LB) to an OD₆₀₀ of 1.0. Cells (1 ml) were collected by centrifugation and

resuspended in 100 μ l of sterile H₂O. Aliquots of 20 μ l of concentrated cells were lysed with 20 μ l of 2 \times SDS sample buffer, heated at 95°C and 10 μ l used for loading. Proteins were separated on denaturing 7.5% SDS–PAGE mini-gels and blotted onto PVDF membranes (0.2 μ m pore size for western blotting; Millipore). Anti- σ^{54} (30) and alkaline phosphatase-conjugated anti-rabbit IgG (Promega) antibodies were used for detection (20).

Protein expression and purification

The R383A and R383K mutant σ^{54} proteins were overexpressed in *E.coli* strain BL21 (pLysS). Freshly transformed *E.coli* BL21 (pLysS) cells (overnight growth) were used to inoculate (~100–200 c.f.u.) 1 l of 2 \times YT medium and grown at 37°C with 50 μ g/ml kanamycin. The cultures were grown to an OD₆₀₀ of between 0.5 and 0.7 and then induced with 1 mM IPTG at 25°C for 2 h. This temperature shift protocol increases the level of solubility of σ^{54} (29) and improves stability of the R383A mutant, which otherwise becomes severely proteolysed when overproduced at higher temperatures. The cells were collected by centrifugation and resuspended in cold 25 mM sodium phosphate (pH 7.0), 0.5 M NaCl, 5% (v/v) glycerol and 1 mM PMSF and lysed in a French press. The lysate was centrifuged at 20 000 g for 30 min and >50% of R383K and ~25% of R383A were found in the soluble fraction. The N-terminal His-tagged mutant proteins were partially purified by Ni affinity chromatography using FPLC and eluted with an imidazole gradient (29). Since R383K and, to a larger extent, R383A co-purified with a truncated form (implying proteolysis of R383K and R383A in the C-terminal domain), peak fractions from the Ni affinity column were dialysed into TGED buffer (10 mM Tris–HCl, pH 8.0, 50 mM NaCl, 0.1 mM EDTA, 1 mM DTT and 5% v/v glycerol) overnight at 4°C for further purification. The truncated fragments in the two protein preparations were removed by heparin and finally Mono Q chromatography essentially as previously described (13). Elution was achieved with a NaCl gradient in both cases. Peak fractions from the Mono Q chromatography were pooled and dialysed against TGED buffer and stored at –70 (long-term storage) or –20°C (short-term storage). Cys383 protein was overexpressed and purified as previously described (18) using a Ni affinity column.

The activator proteins *E.coli* PspF Δ HTH and *K.pneumoniae* NtrC were overexpressed and purified as His₆-tagged fusion proteins from pMJ15 (31) and pDW78 (provided by David Widdick and Ray Dixon). PspF Δ HTH was stored at –70°C in TGED buffer with 50% (v/v) glycerol and NtrC in TGED buffer with 10% glycerol (50 mM Tris–HCl, pH 8.0, 300 mM NaCl, 20 mM imidazole and 10% v/v glycerol). *Escherichia coli* core RNAP was purchased from Epicentre Technologies.

Assay for free sulfhydryl groups (CPM test)

A modified version of the method of Parvari *et al.* (32) was used. Briefly, β -mercaptoethanol standard solutions were prepared in MOPS buffer (10 mM MOPS pH 8.0, 0.1 mM EDTA and 50 mM NaCl) at concentrations of 100, 50, 20, 10, 5, 1, 0.5 and 0.1 μ M. Cys383 was exchanged into MOPS buffer by dialysis at 4°C and protein concentration was determined by Bradford assay. A 15 μ l aliquot of 0.4 mM 7-diethylamino-3-[4'-maleimidylphenyl]-4-methylcoumarin (CPM) in dimethylformamide was added to 15 μ l of each standard and

Table 1. *Escherichia coli glnHp2* and *S.meliloti nifH* promoter sequences.

Promoter	Plasmid	Sequence	Reference
		-28 -13 +1	
<i>E.coli glnHp2</i>	pFC50	ACTGGCACGATTTTT <u>I</u> CATATATGTGAATGT	34
	pFC50-m12	ACTGGCACGATTTTT <u>G</u> CATATATGTGAATGT	34
	pFC50-m33	ACTGGCACGATTTTT <u>C</u> CATATATGTGAATGT	34
	pFC50-m11	ACTGGCACGATTTTT <u>A</u> CATATATGTGAATGT	34
		-29 -14 +1	
<i>S.meliloti nifH</i>	pMKC28	GCTGGCAGACTTTT <u>G</u> CACGATCAGCCCTGGG	36
		-28 -13 +1	
<i>K.pneumoniae glnAp2</i>	–	GTTGGCAGATTT <u>C</u> GCTTTATATTTTAA	

The *E.coli glnHp2* (shown from –28 to +3) and *S.meliloti nifH* (shown from –29 to +3) promoter sequences used for the *in vitro* transcription assays. The –13GC (for the *glnHp2* promoters) and –14GC (for the *nifH* promoter) promoter elements are underlined and the consensus G is shown in bold. The *K.pneumoniae glnAp2* promoter sequence (from –28 to +3) is also given for comparison.

each protein sample. After 1 h incubation at 37°C the reaction was stopped by adding 3 ml of 1% (v/v) Triton X-100. The intensity of fluorescence emission was measured on 1 ml samples, using a Perkin-Elmer 2000 fluorescence spectrophotometer. The excitation wavelength was 390 nm and the emission wavelength was 473 nm.

Core RNAP binding assays

These were performed essentially as previously described as 10 µl reactions in Tris–NaCl buffer (40 mM Tris–HCl pH 8.0, 10% v/v glycerol, 0.1 mM EDTA, 1 mM DTT and 100 mM NaCl) (29). Briefly, *E.coli* core RNAP (250 nM) and different amounts of mutant σ^{54} proteins were mixed together and incubated at 30°C for 10 min, followed by addition of glycerol–bromophenol blue loading dye. Aliquots of 10 µl of the samples were loaded onto Bio-Rad native 4.5% polyacrylamide Mini-Protean II gels and run at 50 V for 2 h at room temperature in Tris–glycine buffer (25 mM Tris and 200 mM glycine). Complexes were visualised by Coomassie blue staining of the gels.

Gel mobility shift assays

³²P-end-labelled, fully complementary 88 bp homoduplex or heteroduplex fragments mismatched at positions –12, –12 to –11, –12 to –6, –12 to –1, –5 to –10 and –10 to –1 (heteroduplexes 1–6, respectively, consisting of the –60 to +28 *S.meliloti nifH* promoter sequence; Table 2) were formed as described (15) and used as probes. *Escherichia coli glnHp2* promoter fragments were obtained by PCR using pFC50 (33) and pFC50-m12 as templates with primers FC5 and FC6 (34). The promoter fragments were gel purified and end-labelled with ³²P. A typical σ^{54} or E σ^{54} (formed with σ^{54} at a 2-fold molar excess over core RNAP) binding assay contained 16 nM DNA and σ^{54} or E σ^{54} (concentrations as indicated in figures or corresponding legends) in STA buffer (25 mM Tris–acetate pH 8.0, 8 mM magnesium acetate, 10 mM KCl, 1 mM DTT and 3.5% w/v PEG 6000) and incubated for 10 min at 30°C. For activation, 4 µM PspFΔHTH activator protein and 4 mM dGTP were used. Briefly, core RNAP, σ^{54} and DNA were pre-incubated at 30°C for 10 min and then nucleotide and activator were added for 10 min and, if required, heparin (final concentration

100 µg/ml) for a further 5 min prior to gel loading. Samples were then loaded onto native 4.5% polyacrylamide gels and run at 60 V for 80 min (for the *E.coli glnHp2* promoter fragments 60 V for 150 min) at room temperature in Tris–glycine buffer. DNA–protein complexes were detected and quantified by phosphorimager analysis.

In vitro transcription assays

The template for transcription assays was either the supercoiled plasmid pMKC28 carrying the *S.meliloti nifH* promoter in pTE103 (35,36) or pFC50 containing the *E.coli glnHp2* promoter and its mutant derivatives (33) harbouring –13 GC element mutations (Table 1): –13T→G (pFC50-m12), –13T→C (pFC50-m33) and –13T→A (pFC50-m11) (the nucleotide numbering system used here is based on *E.coli glnHp2* and differs from that used for *S.meliloti nifH* due to minor variations in the location of the transcription start site; Table 1). The transcription assays were performed in STA buffer as previously outlined (35), except that 30 nM E σ^{54} (30 nM core RNAP:120 nM σ^{54}) and 10 nM DNA was used. For activation, 4 µM PspFΔHTH or 100 nM NtrC were added with 4 mM ATP (plus 10 mM carbamyl phosphate, used for NtrC phosphorylation). The reactions were incubated for 20 min to allow open complexes to form. The remaining rNTPs (100 nM), 3 µCi [α -³²P]UTP and heparin (100 µg/ml) were added and incubated for a further 20 min at 30°C. The reactions were stopped with 4 µl of formamide loading buffer and 7 µl aliquots were loaded on 6% denaturing sequencing gels. The dried gel was analysed on a phosphorimager.

DNA cleavage of the *S.meliloti nifH* promoter DNA

DNA cleavage was conducted essentially as previously described (28). Briefly, closed complexes were formed with 100 nM holoenzyme (ratio 1:2, core RNAP to FeBABE-modified σ^{54}) and incubated at 30°C for 10 min. Cleavage was initiated by rapid sequential addition of 2 mM sodium ascorbate (pH 7.0) and 1 mM hydrogen peroxide. Reactions were allowed to proceed at 30°C for 10 min before quenching with 30 µl of stop buffer (0.1 M thiourea and 100 µg/ml sonicated salmon sperm DNA) and 80 µl of TE buffer (10 mM Tris–HCl pH 8.0, and 1 mM EDTA pH 8.0). The stopped reactions were

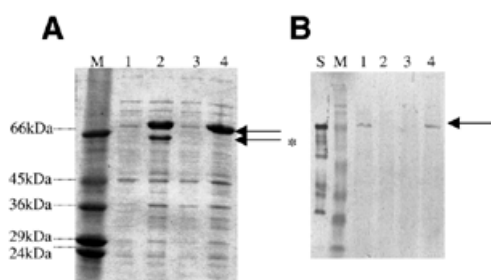


Figure 1. Overexpression and *in vivo* stability of R383K and R383A mutant σ^{54} proteins. (A) Uninduced whole cell extracts from *E. coli* BL21 pLysS carrying pSRW-R383A (lane 1) and pSRW-R383K (lane 3). The arrow indicates expression of R383A (lane 2) and R383K (lane 4) in whole cell extracts after 2 h induction. The arrow with asterisk indicates the proteolysed R383A protein (lane 2). The marker (lane M) is BroadRange SDS-7L (Sigma). (B) Whole cell extracts from *E. coli* strain TH1 carrying pMTH σ (lane 1), pET28b⁺ (lane 2), pSRW-R383A (lane 3) or pSRW-R383K (lane 4) were probed with anti- σ^{54} antibodies. The arrow indicates σ^{54} . The prestained marker M (lane M) is from BioRad (broad range) and lane S contains a partially purified sample of σ^{54} .

phenol/chloroform extracted, precipitated with ethanol and electrophoresed on 10% denaturing urea–polyacrylamide gels. The cleavage sites were determined using end-labelled fragments of the *S. meliloti nifH* promoter DNA.

RESULTS

Expression and stability of the R383K and R383A σ^{54} mutant proteins

We constructed the σ^{54} mutants R383K and R383A to explore their activities *in vitro*. Denaturing gel analysis of whole cell extracts from induced *E. coli* BL21 (pLysS) cultures revealed proteolysis of the overexpressed R383A protein (Fig. 1A, lane 2). In contrast, the R383K protein, harbouring the more conservative substitution, appeared to be more stable and migrated mainly as a single band, as did the wild-type protein during denaturing gel electrophoresis (Fig. 1A, lane 4). Overexpression of the R383A protein in different *E. coli* backgrounds and altering overexpression conditions (time and temperature) did not improve the stability of the R383A protein (data not shown). Since the truncated R383A co-purified with full-length R383A protein during Ni affinity chromatography, R383A appears to be proteolysed in its C-terminal domain. These observations indicate that R383 is structurally important, not readily predicted from the suggestion that R383 is solvent exposed (14). We therefore constructed the R383C mutant protein in a cysteine-free σ^{54} background to measure solvent accessibility (18). The CPM reactivity of R383C in its native state showed that R383C is indeed solvent accessible. Furthermore, the R383C protein was more stable upon overexpression and more active in transcription *in vitro* than were R383A and R383K (18; data not shown). We therefore infer that R383 has a structural role related to the bulk of the side chain and that 383 is a surface accessible residue.

Previous *in vivo* studies led to the conclusion that R383A is unable to initiate transcription from the *E. coli glnAp2* promoter (14). The instability of R383A we observed (Fig. 1A) suggested that the apparent inactivity of the R383A protein

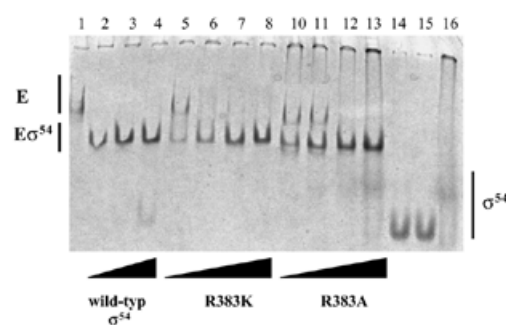


Figure 2. Binding of σ^{54} to *E. coli* core RNAP. Native gel holoenzyme assembly assays were used to detect complexes forming between core RNAP and R383K and R383A, respectively. The formation of holoenzyme ($E\sigma^{54}$) was detected as the presence of a faster migrating species when compared with core (E, lane 1) alone. Titrations of core RNAP with σ^{54} were carried out using 250 nM core RNAP and increasing concentrations of σ^{54} at ratios of 1:1 (lanes 2, 5 and 10), 1:2 (lanes 3, 6 and 11), 1:4 (lanes 4, 7 and 12) and 1:8 (lanes 8 and 13). Wild-type σ^{54} shifted nearly all the core into the holoenzyme form at a 1:1 molar ratio of core to σ^{54} (lane 2); in contrast, R383K shifted all the core to the holoenzyme form at a ratio of 1:2 (lane 6) and R383A at 1:4 (lane 12). Free σ^{54} (2.5 μ M) proteins are also shown: lane 14, wild-type; lane 15, R383K; lane 16, R383A.

could be due to proteolytic cleavage *in vivo* rather than solely a functional defect caused by the mutation. We therefore conducted *in vivo* promoter activation assays (β -galactosidase promoter fusion assays) and western blots with the R383A protein. Leaky expression of *rpoN* in pET28b+ allows use of the overexpression plasmid in these assays (20). Consistent with the previous *in vivo* results (14), the R383A mutant did not support activation *in vivo* (data not shown). Analysis of whole cell extracts containing pSRW-R383A prepared from *E. coli* TH1 cells under activating conditions with anti- σ^{54} polyclonal antibodies failed to detect full-length R383A σ^{54} protein (Fig. 1B, lane 3); wild-type and R383K proteins were detected (Fig. 1B, lanes 1 and 4). It appears that the activity of R383A may not be easily judged by *in vivo* activity assays. We therefore conducted a series of *in vitro* assays to explore the activity of the R383A and R383K mutants.

Interaction of R383K and R383A with the *E. coli* core RNAP

Native gel holoenzyme assembly assays were used to detect complexes forming between core RNAP and σ^{54} based on the different mobilities of core versus holoenzyme. Results showed that R383K has a slightly reduced affinity for core RNAP (Fig. 2). In contrast, R383A had a significantly reduced affinity and, compared to wild-type σ^{54} , forms a holoenzyme with an increased mobility on native gels. The R383A protein did not produce a characteristic σ^{54} band but was diffuse and slower running (Fig. 2, lane 16), in contrast to the R383K and wild-type proteins (Fig. 2, lanes 14 and 15). Previously we showed, using Cys383-tethered FeBABA footprinting methods, that R383 is not proximal to the core subunits β and β' (18). We conclude that changing the invariant R383 to A results in a conformational change that may not be localised and which results in significant changes in core RNAP binding and in formation of holoenzyme with a different conformation. These observations further support a structural role for R383.

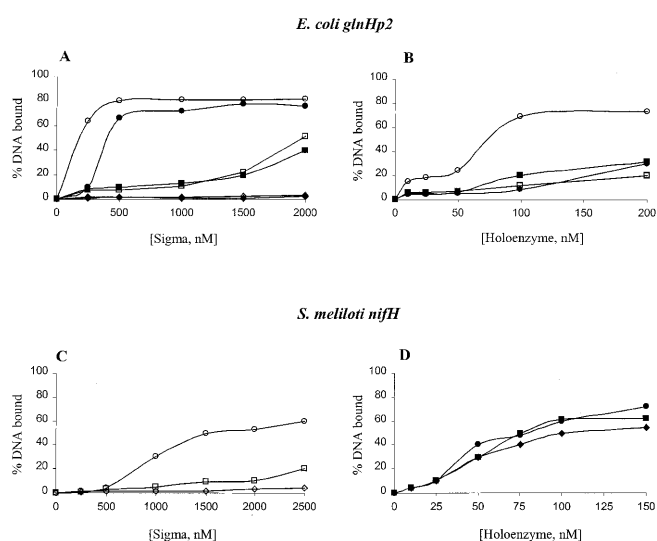


Figure 3. Interactions of R383K and R383A with *E. coli glnHp2* and *S. meliloti nifH* promoter fragments. Gel mobility shift assays were used to detect the binding activities of the σ mutants and their holoenzymes to *E. coli glnHp2* promoter fragments. Binding of (A) wild-type σ^{54} (closed circles), R383K (closed squares) and R383A (closed diamonds) and (B) their holoenzymes to Hp2-13T (closed symbols) and Hp2-13T→G (open symbols). Binding of (C) wild-type σ^{54} (open circles), R383K (open squares) and R383A (open diamonds) and (D) their holoenzymes [as in (C), but with closed symbols] to the *S. meliloti nifH* promoter fragment.

DNA-binding activities of the R383K and R383A mutant σ^{54} proteins and their holoenzymes

The R383K mutant was suggested to show an altered DNA-binding preference for the promoter GC element (14). Using a gel mobility shift assay we compared the DNA-binding activities of the R383A, R383K and wild-type σ^{54} proteins and their holoenzymes for *E. coli glnHp2* (termed Hp2-13T) and a mutant derivative with a T→G substitution at position -13 (termed Hp2-13T→G) (Fig. 3A and B, respectively). The *glnHp2* promoter is very close in sequence to the *K. pneumoniae glnAp2* promoter used in previous *in vivo* work with R383 mutants (14; Table 1). Previous *in vivo* and *in vitro* studies have shown that the *glnHp2* promoter with a G at -13 is a better substrate for σ^{54} holoenzyme function than one with a T at -13 (33). Binding of σ^{54} confirmed the promoter with a G at position -13 (Hp2-13T→G) as the preferred template, to which σ^{54} had 7-fold increased binding (at 250 nM) compared to the Hp2-13T promoter. The R383K mutant bound both promoter sequences similarly, but had a 7- to 8-fold reduced overall binding (at 1 μ M) to the Hp2-13T and Hp2-13T→G templates compared to wild-type σ^{54} (Fig. 3A). This observation, together with the inability of R383A to detectably bind either promoter probe even at higher protein concentrations (1.5 and 2 μ M; Fig. 3A) establishes that R383 is important for DNA binding by σ^{54} .

By comparing the binding activities of the wild-type, R383A and R383K holoenzymes for the two promoter probes we determined that the wild-type holoenzyme (at 100 nM) had a 4- to 5-fold higher binding to the Hp2-13T→G than the Hp2-13T promoter sequence (Fig. 3B). The biphasic nature of the graph in Figure 3B (wild-type holoenzyme binding to Hp2-13T→G) probably reflects the complex binding mode of σ^{54}

holoenzyme to DNA. Like R383K σ^{54} , the R383K holoenzyme showed a similar binding preference to both promoter probes, being unable to distinguish between them (Fig. 3B). Clearly, σ^{54} -core RNAP interactions are significant in determining promoter binding (compare Fig. 3A and B) and it seems that σ^{54} dominates the promoter binding preference. Any binding preferences of the R383A holoenzyme for Hp2-13T and Hp2-13T→G could not be determined due to low binding of the R383A holoenzyme to both probes (data not shown). Overall, our data show that R383K and its holoenzyme bind the Hp2-13T→G and Hp2-13T templates equally. In contrast, wild-type σ^{54} and its holoenzyme bind to the Hp2-13T→G probe better than to the Hp2-13T probe. R383 is significant for DNA binding by σ^{54} and is needed for preferential binding to -13G rather than the -13T probe.

To further explore the DNA-binding properties of the mutant σ^{54} proteins and their holoenzymes we compared the binding activities of R383K and R383A to *S. meliloti nifH* promoter DNA, a higher affinity binding site used for many σ^{54} activity measurements (see below). As shown (Fig. 3C), R383K bound less *S. meliloti nifH* probe (3-fold reduced) compared to wild-type σ^{54} . In contrast, the R383A mutant appeared defective for DNA binding. Next, holoenzyme binding to the *S. meliloti nifH* promoter was assayed using saturating ratios of σ to core RNAP. The wild-type holoenzyme shifted 70% of the *S. meliloti nifH* promoter probe DNA at 150 nM, whereas mutant holoenzymes shifted 60 (R383K) and 45% (R383A) of the probe (Fig. 3D). This observation contrasts with the behaviour of the R383A holoenzyme on Hp2-13T→G and suggests that sequences in the *S. meliloti nifH* promoter rescue promoter binding by R383A holoenzyme.

In vitro transcription activity of the R383K and R383A holoenzymes

To begin to examine the consequences of altered DNA binding by R383K and R383A upon later steps in activation, we next examined the ability of the R383K and R383A holoenzymes to support transcription *in vitro* from supercoiled plasmid pFC50, which contains the wild-type *E. coli glnHp2* promoter or GC promoter region mutant derivatives of this promoter (Table 1). Changing -13T to a C (pFC50-m33) or A (pFC50-m11) results in a strong promoter-down phenotype or a largely inactive mutant promoter, respectively (33).

Initially, the response of wild-type and mutant holoenzymes to saturating concentrations of the *E. coli* activator protein PspF Δ HTH, which functions in solution, was tested. The ability of the holoenzymes to promote transcription at *glnHp2*-13T, *glnHp2*-13T→G and *glnHp2*-13T→C was expressed as a percentage of wild-type holoenzyme activity at the *glnHp2*-13T→G promoter (Fig. 4A). Assays were conducted with sub-saturating amounts of holoenzyme to allow quantitative detection of holoenzyme activities (see Materials and Methods). Experiments were performed at least six times to enhance reliability. The standard error range for the data shown in Figure 4A and B was $\pm 4\%$. The results clearly show that the R383A holoenzyme is active and able to support transcription *in vitro* (40–50% of wild-type activity on the *glnHp2*-13T→G promoter; Fig. 4A). Transcription by R383A is apparently greater than promoter DNA binding by the holoenzyme (Fig. 3B). Formation of stable open complexes

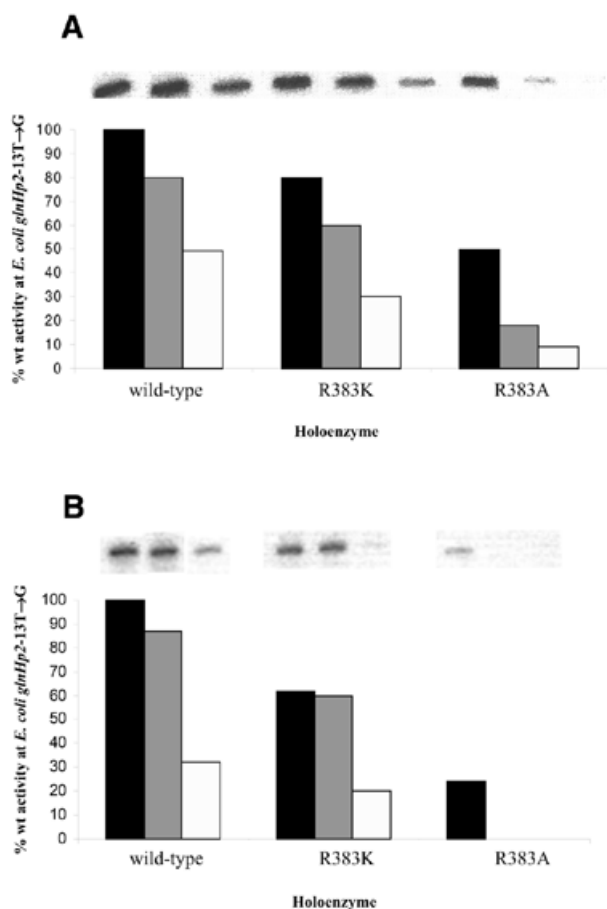


Figure 4. *In vitro* activator-dependent transcription assays on *E. coli glnHp2* wild-type and mutant promoter sequences. The sequences of the promoters used for transcription are as shown in Table 1. (A) PspF Δ HTH-activated transcription and (B) NtrC-activated transcription on *glnHp2*-13T→G (pFC50-m12) (black bars), *glnHp2*-13T (pFC50) (grey bars) and *glnHp2*-13T→C (pFC50-m33) (white bars). The transcription activities are expressed as a percentage of wild-type activity at the *glnHp2*-13T→G (pFC50-m12) promoter.

that do not rapidly decay to heparin-sensitive closed complexes could explain this.

The R383K holoenzyme was $20 \pm 4\%$ less efficient in transcription than the wild-type holoenzyme at all the promoters tested (Fig. 4A). This result differs from the *in vivo* assays on *K. pneumoniae glnAp2* (Table 1), which showed that the R383K holoenzyme transcribed better from -13T or -13T→C promoters than did wild-type σ^{54} (14). To explore the potential for suppression *in vitro* we varied the assay conditions. We failed to see any significant R383K-specific suppression at the promoter-down mutant (*glnHp2*-13T and *glnHp2*-13T→C) sequences in the presence of nucleotides that facilitate formation of initiated complexes prior to heparin challenge, at higher temperatures (37 instead of 30°C) used to stimulate transient DNA melting, at different (10–8000 nM) PspF Δ HTH concentrations or with varying incubation times (5, 10, 20 and 30 min) before and after addition of heparin (data not shown).

The possibility that the suppression of promoter-down *K. pneumoniae glnAp2* mutants by R383K seen *in vivo* could be either activator-specific or require an enhancer-bound activator was considered. We used NtrC instead of PspF Δ HTH

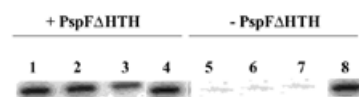


Figure 5. *In vitro* activator-independent transcription assays on the *E. coli glnHp2*-13T→G (pFC50-m12) promoter. Activator-dependent (lanes 1–3) and activator-independent ‘bypass’ transcription (lanes 5–7) for wild-type σ^{54} , R383K and R383A, respectively, are shown. The R383A mutant σ^{54} (35) was used as the positive control in both cases (lane 4 for activator-dependent and lane 8 for activator-independent reactions).

and examined *in vitro* transcription activity of the wild-type and mutant holoenzymes at the *glnHp2* promoters. The results showed that when activated by NtrC, the R383K holoenzyme transcribed from the *glnHp2*-13T and *glnHp2*-13T→G promoters at levels consistent with our observation using *glnHp2*-13T→G and PspF Δ HTH (compare Fig. 4A and B). In contrast to the PspF Δ HTH results, a much lower activity of R383A holoenzyme at the *glnHp2*-13T→G or no detectable activity at the *glnHp2*-13T and *glnHp2*-13T→C promoters, even at higher holoenzyme and NtrC concentrations (data not shown), was evident. This could be linked to an altered holoenzyme conformation (Fig. 2) and reduced DNA binding by the R383A holoenzyme (Fig. 3B).

In conclusion, our *in vitro* transcription results do not show the suppression of promoter-down phenotypes of the *E. coli glnHp2* promoter by R383K holoenzyme reported for *in vivo K. pneumoniae glnAp2* promoter assays (14). The *in vitro* activities of the R383K and R383A holoenzymes argue that R383, at least *in vitro*, is not absolutely required for productive transcription initiation by $E\sigma^{54}$. It seems that R383 is not needed to allow preferential initiation of transcription in which the -13 base is G rather than T (Fig. 4).

Activator-independent transcription activity of the R383K and R383A holoenzymes

Maintaining the transcriptionally silent state of $E\sigma^{54}$ in closed complexes depends upon the interaction of σ^{54} with locally distorted promoter DNA downstream of the consensus -12 GC promoter element (10,26,27). σ^{54} proteins defective in recognition of the -12 GC promoter element proximal DNA distortion are capable of increased activator-independent transcription *in vitro*, so called bypass transcription (8,20,25). We used the *in vitro* bypass assay to see whether holoenzymes formed with R383K and R383A were active in unregulated transcription from the *glnHp2*-13T→G promoter. We used R383A mutant σ^{54} as a positive control for the bypass transcription assay (35) and PspF Δ HTH for activator-dependent transcript formation. As shown, no bypass transcription was observed with R383K or R383A (Fig. 5). Additional assays from *glnHp2*-13 variants (33) or pMKC28 carrying the *S. meliloti nifH* promoter (33) failed to give unregulated transcription with the R383 mutants (data not shown). The failure to detect bypass transcription with R383K and R383A suggests tight binding of these mutant σ^{54} proteins to the early melted DNA formed in closed complexes, as seen in heteroduplex DNA-binding assays (25,27). Bypass transcription correlates with strong defects in the binding of σ^{54} to early melted DNA, a defect that is only weakly evident with the R383 mutants (see below). Thus we infer that the R383A and R383K mutants appear functionally

Table 2. The *S.meliloti nifH* and *E.coli glnHp2* DNA fragments used for the gel mobility shift assays

Heteroduplex	Sequence
1	-12 -60...GCTGGCAGACTTTT GC CGATCAGCCCTGGG...+28
2	-12 to -11 -60...GCTGGCAGACTTTT GC CAGATCAGCCCTGGG...+28
3	-12 to -6 -60...GCTGGCAGACTTTT GC CATCGACGCCCTGGG...+28
4	-12 to -1 -60...GCTGGCAGACTTTT GC CATCGACTAAAGGGG...+28
5	-10 to -1 -60...GCTGGCAGACTTTT GC ACTCGACTAAAGGGG...+28
6	-5 to -1 -60...GCTGGCAGACTTTT GC ACGATCA TAAAGGGG ...+28
7	wild-type -60...GCTGGCAGACTTTT GC CAGATCAGCCCTGGG...+28
<hr/>	
<i>glnHp2</i> -13T→G(-12)	-60...ACTGGCAGACTTTT GC TATATGTGAATGT...+28

The *S.meliloti nifH* and *E.coli glnHp2*-13T→G (-12) heteroduplex promoter DNA fragments (from -60 to +28) used for the gel mobility shift assays. Shown are sequences from -26 to +3, where the σ^{54} consensus promoter sequences are in bold and mutant sequences introduced in the top strand to create the mismatch are boxed in black (16,27).

intact in the generation and maintenance of locally melted -12 proximal promoter structures associated with the closed complex (8,25). Further, chemical footprinting with copper *o*-phenanthroline of closed complexes formed with R383 mutant holoenzymes revealed a local distortion of promoter DNA 3' adjacent to the GC element, as seen with the wild-type holoenzyme but not in bypass mutants (26,35; data not shown). Overall, R383 is neither directly nor indirectly associated with inhibition of unregulated bypass transcription *in vitro*. By inference, R383 does not closely interact with the elements of the -12 promoter region that are involved in maintaining the stable conformation of the closed complex and in limiting DNA opening prior to activation.

Interaction of R383K and R383A mutant proteins and their holoenzymes with heteroduplex *S.meliloti nifH* promoter DNA probes

In the course of the *in vitro* transcription experiments we observed that the R383K and R383A holoenzymes were essentially inactive for transcription at the *S.meliloti nifH* promoter even though promoter binding was sufficiently efficient to expect transcripts (Fig. 3D and data not shown, respectively). The transcriptional inactivity of the mutant proteins at the *nifH* promoter but not at the *glnHp2*-13T→G promoter with essentially the same -12 region sequences (Table 1) prompted us to further explore the properties of the R383K and R383A mutant proteins. *Sinorhizobium meliloti nifH* (from -11 to -1) is rich in G and C residues, whereas *E.coli glnHp2*, like the *K.pneumoniae glnAp2* promoter used in the *in vivo* assays, is AT-rich in this region, which is melted in open complexes (Table 1). This led us to consider that the R383K and R383A mutant holoenzymes might be defective in some aspect of DNA melting or single-stranded DNA binding at the *S.meliloti nifH* promoter. We used heteroduplex DNA that mimics the DNA at different stages of open complex formation to test this idea (Table 2). In marked contrast to the failure to transcribe

from the *S.meliloti nifH* promoter (data not shown), both the R383K and R383A mutant holoenzymes gave heparin-stable, activator- and nucleotide hydrolysis-dependent complexes on promoters with a region of heteroduplex from -10 to -1 (Table 2, heteroduplex 5) (Fig. 6A). On this DNA structure the mismatched region includes the non-conserved sequence from -10 to -1 that interacts with σ^{54} within the closed complex (13) or with σ^{54} holoenzyme in the open promoter complex (37-39). The ability of the wild-type, R383K and R383A holoenzymes to form activator- and nucleotide hydrolysis-dependent, heparin-stable complexes when bound to promoter DNA where the sequence from -10 to -1 is heteroduplex (Table 2, heteroduplex 5) argues that the R383K and R383A holoenzymes are not *per se* defective in polymerase isomerisation at the *nifH* promoter. Also, pre-opening from -10 to -1 appears to allow a range of activities with R383K and R383A similar to that seen with the *glnHp2* promoters in transcription assays. As expected from the *in vitro* activator-dependent transcription results, the wild-type holoenzyme, like the R383K and R383A holoenzymes, does not form heparin-stable, activator- and nucleotide hydrolysis-independent complexes on heteroduplex 5 (16; data not shown).

Heteroduplex with early melted sequences. Next we examined whether the R383A and R383K mutants were defective in interacting with DNA structures representing the early stages of DNA melting. We used heteroduplex promoter DNA fragments unpaired at -12 (Table 2, heteroduplex 1) and at -12/-11 (Table 2, heteroduplex 2) to mimic the structure believed to be involved in initial DNA opening (25,27). These heteroduplexes allow the wild-type holoenzyme to form complexes that survive a heparin challenge independently of activator and nucleotide hydrolysis (25). As shown (Fig. 6B), we were unable to form heparin-stable complexes with the R383K and R383A holoenzymes on either of the heteroduplexes, even under activating conditions. This defect correlates with the

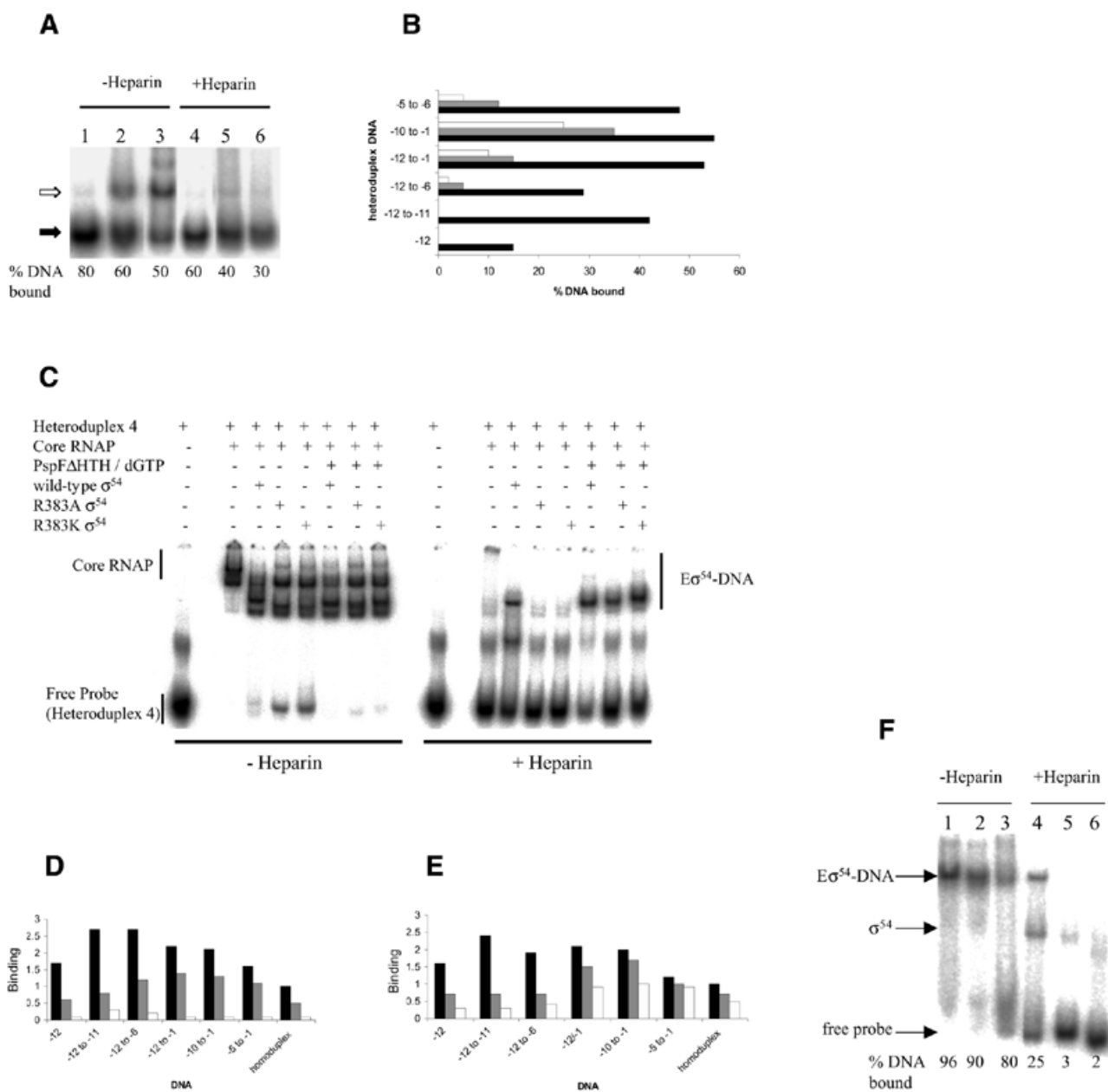


Figure 6. Binding of R383K and R383A to homo- and heteroduplex promoter DNA probes. **(A)** Activator- and nucleotide-dependent, heparin-resistant open complex formation on the *S. meliloti nifH* heteroduplex -10 to -1 (heteroduplex 5, Table 2) by wild-type σ^{54} (lane 1), R383K (lane 2) and R383A (lane 3) holoenzymes (100 nM). Black arrows indicate the position of the $E\sigma^{54}$ -DNA complex; white arrows the position of core RNAP complex. Reactions without (lanes 1–3) and with (lanes 4–6) heparin (100 μ g/ml) challenge for 5 min prior to loading are shown. **(B)** Activator-dependent, heparin-resistant $E\sigma^{54}$ -DNA complex formation on heteroduplexes (heteroduplexes 1–6, Table 2). Percent DNA shifted with the wild-type σ^{54} (black bars), R383K (grey bars) and R383A (white bars) holoenzymes are shown. **(C)** Stability of wild-type and mutant $E\sigma^{54}$ -DNA complexes on *S. meliloti nifH* heteroduplex -12 to -1 (heteroduplex 4) under non-activating and activating conditions in the presence and absence of heparin (100 μ g/ml), respectively (lanes as indicated on figure). The slower running band in the lanes containing $E\sigma^{54}$ is a heparin-unstable complex of $E\sigma^{54}$ with DNA (15,35,40). **(D)** DNA-binding activities of R383K (grey bars) and R383A (white bars) to homo- and heteroduplex DNA (see Table 2) expressed as a fraction of wild-type σ^{54} (black bars) binding. **(E)** As (D) but for holoenzymes. **(F)** Activator- and nucleotide hydrolysis-independent, heparin-stable $E\sigma^{54}$ -DNA complex formation on *E. coli glnHp2-13T \rightarrow $G(-12)$ (see Table 2). Reactions without (lanes 1–3) and with (lanes 4–6) heparin challenge are shown. Lanes 1 and 4, wild-type σ^{54} ; lanes 2 and 5, R383K; lanes 3 and 6, R383A.*

inability of the R383 mutants to transcribe from the *nifH* promoter. However, when using heteroduplex promoter DNA where the sequences from -12 to -6 (Table 2, heteroduplex 3) and -12 to -1 (Table 2, heteroduplex 4) were unpaired, the R383K and R383A holoenzymes survived the heparin challenge, but only with activator and nucleotide hydrolysis

(compare Fig. 6B and C). In contrast, the wild-type holoenzyme formed heparin-stable complexes on heteroduplex 4 in the absence of activator and nucleotide, as predicted from the results with heteroduplexes 1 and 2, opened at -12 (Table 2, heteroduplex 1) and from -12 to -11 (Table 2, heteroduplex 2) (16,25,27,40). Although non-native structures near -12 have

the property of allowing the wild-type holoenzyme to form heparin-stable complexes independently of activation, the R383K and R383A holoenzymes formed heparin-stable and activator- and nucleotide hydrolysis-dependent complexes with promoter probes containing -12 proximal melts (Table 2, heteroduplexes 1 and 2) only when these heteroduplexes included further regions of heteroduplex proximal to the start site (Table 2, heteroduplexes 3 and 4). These results show that R383 specifies an interaction in the closed complex associated with stable complex formation by the holoenzyme when the -12 proximal sequences are melted. Other interactions required to acquire heparin-stable complex formation involving late melted sequences appear intact in the R383K and R383A mutants.

DNA-binding activities on heteroduplexes. Next, we measured the DNA-binding activities of the mutant proteins (Fig. 6D) and their holoenzymes (Fig. 6E) on *S.meliloti nifH* heteroduplex DNA with -12 promoter element proximal melts (Table 2, heteroduplexes 1 and 2), start site proximal melts (Table 2, heteroduplexes 3 and 4) and on heteroduplexes with mismatches between -10 and -1 (Table 2, heteroduplex 5) and -5 to -1 (Table 2, heteroduplex 6). Results are shown relative to binding of wild-type σ^{54} and its holoenzyme to *S.meliloti nifH* homoduplex DNA. It is evident that R383K and, especially, its holoenzyme bound more (2- to 3-fold) of the heteroduplex DNA probes which contain start site proximal melts, whilst wild-type σ^{54} and its holoenzyme prefer heteroduplex DNA with -12 proximal melts. Since certain Region I mutants of σ^{54} have defects in binding to early melted DNA structures (8,25,27), the DNA-binding properties of R383 mutants (Fig. 6) may reflect indirect effects upon the function of Region I (28).

The results (Fig. 6) clearly imply a role for R383 in interactions within the closed complexes in which limited DNA opening next to the -12 element has occurred. To further explore this idea we used the *E.coli glnHp2-13T*→G promoter mismatched at position -11 (i.e. *glnHp2-13T*→G equivalent to heteroduplex 1; Table 2). R383K had 80% of wild-type transcription activity on this promoter *in vitro*. As shown (Fig. 6F), whilst the wild-type holoenzyme was able to form activator- and nucleotide hydrolysis-independent, heparin-stable complexes on the *glnHp2* heteroduplex, the R383K holoenzyme did not. Activation enabled the R383K and, to a lesser extent, R383A holoenzymes to form some heparin-stable complexes (<10% DNA shifted) on this heteroduplex (data not shown). The ease of opening of the *glnHp2* AT-rich sequence (from -11 to -1) may explain why the activator allows acquisition of heparin stability, and also why a longer segment of heteroduplex is needed at *nifH*. Therefore, binding assays with two different σ^{54} -dependent promoters are consistent with the view that R383 has a role in interactions within the initial closed complexes in which limited DNA opening next to the -12 element has occurred. Unless DNA opening occurs easily, the defects associated with R383 dominate and few open complexes form.

Proximity of residue 383 to promoter DNA

To examine the physical proximity of R383 to promoter DNA we constructed a σ^{54} with FeBABE located at 383. A single cysteine substitution at 383 was made, the naturally occurring

cysteines of *K.pneumoniae* σ^{54} at 198 and 346 having been replaced by alanine to allow 383-specific conjugation of FeBABE. DNA cleavage by tethered FeBABE is achieved through the generation of hydroxyl radicals coordinated to the Fe^{2+} , which attack the deoxyribose-sugar backbone of nucleic acids within a radius of 12 Å from the FeBABE attachment site (reviewed in 41). Using the *S.meliloti nifH* homoduplex DNA probe the DNA-binding activity of the R383C mutant was 90% that of the wild-type and Cys-free σ^{54} activity (data not shown). Upon conjugation with FeBABE (76% efficiency) the DNA-binding activity remained largely unchanged. This suggests that even a relatively bulky substituent at 383 is tolerated for DNA binding, consistent with R383 being dispensable for DNA binding (this paper) and non-essential for transcription (this paper; 18). σ^{54} containing Cys383-tethered FeBABE failed to produce detectable cutting of several different *S.meliloti nifH* promoter templates (homoduplex and heteroduplexes 2 and 5), both in the presence and absence of core RNAP and under activating conditions that allow open complex formation (see below and data not shown). We considered the possibility that σ^{54} containing Cys383-tethered FeBABE and its holoenzyme might have dissociated from the promoter DNA under DNA cleavage conditions. However, binding assays conducted with the Cys383-tethered FeBABE protein under DNA cleavage conditions showed that 91% of σ^{54} containing Cys383-tethered FeBABE and 48% of holoenzyme containing Cys383-tethered FeBABE remained bound to DNA (Fig. 7A). Repeated experiments failed to show DNA cutting by σ^{54} containing Cys383-tethered FeBABE and its holoenzyme. As one positive control σ^{54} with FeBABE conjugated to Cys346, at the edge of the DNA cross-linking patch of σ^{54} , produced cutting proximal to the GC element on *S.meliloti nifH* homoduplex promoter DNA (Fig. 7B). The putative HTH motif in σ^{54} is C-terminal to a patch of amino acids that UV cross-links to promoter DNA. In this patch FeBABE conjugated to residue 336 cut DNA downstream of the conserved GC promoter element (28). As shown in Figure 7B, holoenzyme containing Cys346-tethered FeBABE strongly cut homoduplex promoter DNA between positions -14 and -7, mostly downstream of the GC element, but this cutting was upstream of that seen with the Cys336-tethered FeBABE derivative (28). The C-terminal to N-terminal orientation of the cross-linking patch is therefore 5'→3' with respect to the template strand of the promoter DNA.

DISCUSSION

Specific recognition of promoter DNA by σ factors has an essential role in locating the RNAP at the correct site for initiation. However, the function of residues in σ^{54} that contact DNA are likely to be more complex than just facilitating promoter location. Emerging functions associated with σ^{54} -DNA binding include recognition of the DNA fork junction created when the DNA starts to melt and keeping the polymerase silent for transcription (8,10,15,35). Protein footprints suggest that the DNA-binding domain of σ^{54} is part of the interface with core RNAP and properties of mutants indicate a role in generating polymerase isomerisation and facilitating promoter opening (7,27,35). Our results address the functions of invariant residue R383 of σ^{54} , previously implicated in interactions with the -12 promoter element (14).

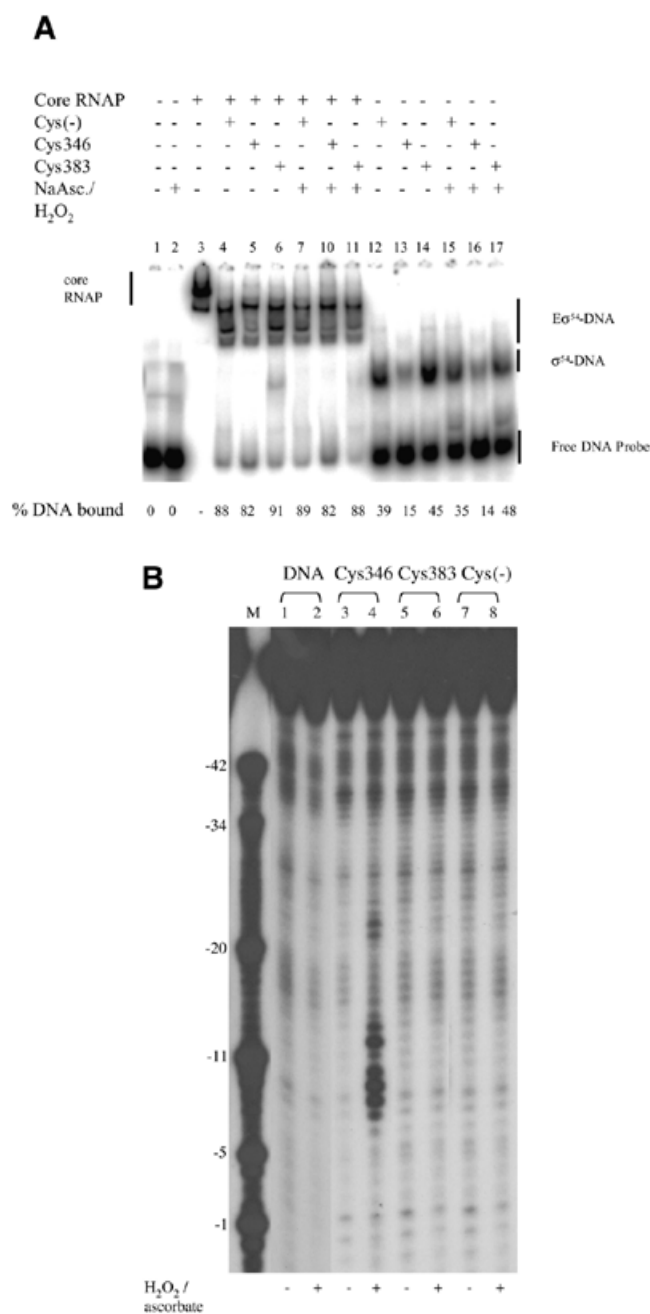


Figure 7. *Sinorhizobium meliloti nifH* promoter DNA template strand cleavage by RNAP holoenzyme containing FeBABA-modified σ^{54} proteins. (A) Cys383-FeBABA σ^{54} and E σ^{54} binding to the *S.meliloti nifH* homoduplex probe under DNA cleavage conditions (lanes as marked on figure). (B) Homoduplex cleavage. Reactions to which hydrogen peroxide and ascorbate were added to initiate DNA cleavage are marked +; control reactions to which no ascorbate and hydrogen peroxide were added are marked -. Lane M contains a mixture of end-labelled *S.meliloti nifH* promoter DNA fragments as molecular weight markers.

Protein stability

R383 is clearly required for protein stability *in vivo*. The instability of R383A may be associated with an unfavourable change in structure directly increasing its proteolytic sensitivity. Alternatively, the reduced DNA-binding activity of R383A may indirectly increase proteolysis by changing the intracellular

location of σ^{54} . The suggestion from *in vivo* promoter activation assays that R383 is essential for σ^{54} function may be incorrect, as purified R383A does support transcription from the *E.coli glnHp2* promoter *in vitro*.

Core RNAP binding

That part of σ^{54} strongly footprinted by the core RNAP is centred on residue 397 and in the absence of Region I ($\Delta I\sigma^{54}$) much of the 325–440 sequence is protected by core RNAP (7). R383A had reduced core RNAP binding and formed a holoenzyme with altered mobility on native gels, suggesting that R383 contributes to core RNAP binding. Possibly, the core interface of σ^{54} is altered in the R383A mutant, potentially in a manner that involves Region I sequences (7,18,19). Interestingly, Cys383-tethered FeBABA footprinting of core RNAP failed to show any proximity of residue 383 (within at least 12 Å) to the core subunits β and β' (18). Thus we suggest that the defects in core RNAP binding by the R383 mutants are indirect. The R383K mutant was less disrupted for core binding, consistent with the conservative nature of the mutation.

DNA binding

Gel mobility shift assays showed that R383A was very defective in DNA binding, R383K less so. R383K did not preferentially bind *E.coli glnHp2*-13T promoter DNA. R383K is reported to transcribe more efficiently than wild-type σ^{54} from a similar promoter sequence (mutant *K.pneumoniae glnAp2*) (14). Clearly, the increased transcription reported may not simply correlate with increased DNA binding of σ^{54} . R383K might therefore influence other steps to allow increased transcription *in vivo*. The R383K holoenzyme did not footprint the *glnAp2*-13G→T promoter *in vivo*, but wild-type σ^{54} did, consistent with the view (developed below) that promoter occupancy may not be dominant for the increased transcription observed (14). It was striking that the defects in *in vitro* transcription at *E.coli glnHp2* with the R383K and R383A mutants were less than the defects in *in vitro* σ and holoenzyme DNA binding. We interpret this to mean that promoter occupancy is not reduced to a point that severely limits transcription *in vitro*. It is plausible that tight binding of the holoenzyme to the promoter increases a transition barrier for open complex formation. The R383K and R383A mutants may reduce this barrier, compensating for reduced promoter occupancy. This favourable effect might contribute to the elevated activities observed with R383K *in vivo* and the good level of transcription detected *in vitro*. It may also partly compensate for the defect in forming stable complexes with early melted DNA (discussed below).

Interactions with heteroduplex DNA

Results from transcription assays with heteroduplexes suggested that slow opening of the DNA at the *S.meliloti nifH* promoter might mean that the closed complex or an activator-dependent isomerised holoenzyme formed with R383K dissociates prior to full strand opening. In contrast, more frequent opening of the *E.coli glnHp2* promoter or stable opening as in heteroduplexes may explain why these templates support stable open complex formation with R383K. Even so, these complexes decay more rapidly than those formed with wild-type σ^{54} (data not shown), suggesting that R383 contributes to DNA binding within the open complex. However, R383 is not

essential for transcription, at least *in vitro*. Our ability to recover activator-dependent stable complex formation using pre-melted *S.meliloti nifH* DNA templates with heteroduplex -10 to -1 sequences suggests that the mutant holoenzymes are limited at some promoters in steps leading to full DNA melting. Compared to DNA templates with start site proximal melts, DNA templates with melted sequences proximal to the -12 promoter element were poor DNA-binding sites for the R383K and R383A mutants. The failure of the R383A and R383K mutants to bind well or make stable complexes on the heteroduplex promoter fragments with -12 proximal melts suggests that the R383 mutant proteins are directly or indirectly defective for interaction with such structures. With the mutant proteins the activator did not allow the use of heteroduplex promoters with -12 proximal melts for efficient stable complex formation on either the *S.meliloti nifH* or *E.coli glnHp2* promoters, but in the context of the *S.meliloti nifH* promoter the activator allowed formation of stable complexes on promoter sequences which were further opened to include the -1 residue. Overall, the results suggest that DNA melting from -10 to -1 stabilises the promoter complexes that form with the R383K and R383A mutant holoenzymes and that the initial melting at -12 is unfavourable for stable σ^{54} -DNA binding when R383 is altered to A or K. Rapid melting at the AT-rich *E.coli glnHp2* may allow stable complexes to form, but slow melting at the GC-rich *S.meliloti nifH* may result in reduced stable complex formation.

Bypass transcription

Interaction of σ^{54} with the -12 GC promoter element appears important in maintaining the transcriptionally silent state of the holoenzyme. Mutations that change the sequences adjacent to the GC or substitution of certain amino acids in σ^{54} that interact with it allow transcription independent of activator (8,20,22,24,42). The σ^{54} DNA-binding domain mutant R336A gives strong bypass transcription (35). R383K and R383A did not, despite supporting levels of activated transcription and binding to -10 to -1 heteroduplex DNA (heteroduplex 5), which suggested that bypass activity might be readily detected. If R383 interacts with the -12 GC promoter sequence, it would appear not to be an interaction contributing to maintaining the silent state of the holoenzyme prior to activation, in contrast to the properties of the R336A and Region I mutants (20,24,35).

DNA proximities

Residue 383 was suggested to be within a HTH motif, expected to establish direct contacts with DNA and thought to interact with the -12 region of the promoter (14). Although our data show that substitutions at 383 influence DNA binding, other data suggest that a simple direct interaction of R383 with DNA may not occur. Cleavage of the promoter DNA by Cys383-tethered FeBABE was not evident. Closed complex promoter DNA cleavage by the FeBABE derivative of σ^{54} in the UV cross-linking patch (Cys336-tethered FeBABE) is centred around position -9 (± 1) (28), while DNA cutting by the Cys346-tethered FeBABE derivative is centred further upstream at position -11 (± 1) (Fig. 7). Given that the UV cross-linking patch is α -helical in structure, the FeBABE cleavage data suggest that the UV cross-linking patch (N-terminal to the HTH motif) aligns with or is inclined towards the

promoter DNA template strand in closed complexes. The lack of any discernible cleavage by the Cys383-tethered FeBABE derivative suggests that either residue 383 is not involved in a direct DNA contact or that some structural consequences of making substitutions at 383 do not allow detection using the FeBABE methodology. However, R383C was active for transcription *in vitro*, more so than R383A (18).

Summary

Overall, our data are consistent with a requirement for R383 to distinguish between T or G at -13 and overall reduced DNA binding when it is substituted by K or A (14). It is possible that some of the overall loss in DNA-binding activity has a basis in an altered protein structure rather than simple loss of a DNA-interacting side chain, a view supported by the *in vivo* instability of R383A. Although instability is unexpected on substitution of a surface exposed residue in an α -helix by alanine, there are suggestions from secondary structure predictions that R383 may exist within a non-helical structure ([www.http://jura.ebi.ac.uk:8888](http://jura.ebi.ac.uk:8888)). The data presented in Figures 1-5 suggest that the interpretation placed on the *in vivo* activation data may need reconsideration and suggest that R383 has a previously unexpected role in the stability of σ^{54} .

In the absence of additional structural or proximity data, any suggestion that the HTH motif lies within a fold that localises sufficiently near the -12 region to contact DNA is speculative. A colinear arrangement, N-terminal to C-terminal (beginning at the -24 promoter element and ending at the start site proximal sequences), of the UV cross-linking patch, the HTH motif and the RpoN box is possible, but unproven. Further, the clear involvement of the σ^{54} Region I sequences in promoter binding has shown that determinants outside the DNA-binding domain make critical contributions to the DNA binding function of σ^{54} (8,20,25,28).

Specialisation of function across the σ^{54} DNA-binding domain is evident. Residues F402, F403, F354 and F355 appear to be associated with interactions needed for efficient polymerase isomerisation (40,43), R383 with forming stable initially melted DNA complexes and R336 with maintaining the inhibited silent state of the polymerase (10,35). We note functional similarities between the putative α -helix, in which C346 and R336 in σ^{54} lie, and helix 14 of *E.coli* σ^{70} . Both helices interact with promoter sequences that include recognition sequences (15,44). They also contain determinants for binding locally single-stranded DNA structures from which melting originates and spreads (8,26,28,45). These and other considerations lead to the view that a series of linked interactions that involve σ^{54} -DNA interaction and σ^{54} -core interfaces are required to change in order to allow the polymerase to progress to the open complex. It seems that the putative HTH motif of σ^{54} contributes as a structural element rather than as a major direct DNA-contacting surface. Nevertheless, several conformational changes in σ^{54} are probably necessary for open complex formation. Transient contacts between σ^{54} and core RNAP or between σ^{54} and promoter DNA may have escaped our analysis of Cys383-tethered FeBABE proximities to DNA. Current data suggest that the centre formed by Region I, the UV cross-linking patch of σ^{54} and the -12 promoter region does not include the HTH motif as an element in proximity (15,18,28).

ACKNOWLEDGEMENTS

We thank Nobuyuki Fujita for help with early stages of this work, Wendy Cannon for oligonucleotides and members of the MB laboratory for comments on the manuscript. This work was supported by a Biotechnology and Biological Sciences Research Council (BBSRC) project grant to M.B. and by a post-graduate studentship from the LEA, Karlsruhe, Germany, to S.R.W.

REFERENCES

- Kelly, M.T. and Hoover, T.R. (2000) The amino terminus of *Salmonella enterica* σ^{54} defective in transcription initiation but not promoter binding activity. *J. Bacteriol.*, **182**, 513–517.
- Lee, J.H. and Hoover, T.R., (1995) Protein cross-linking studies suggest that *Rhizobium meliloti* C-4-dicarboxylic acid transport protein-D, a σ^{54} -dependent transcriptional activator, interacts with σ^{54} -subunit and the β -subunit of the RNA-polymerase. *Proc. Natl Acad. Sci. USA*, **92**, 9702–9706.
- Rippe, K., Guthold, M., von Hippel, P.H. and Bustamante, C. (1997) Transcriptional activation via DNA-looping: visualization of intermediates in the activation pathway of *E. coli* RNA polymerase and σ^{54} holoenzyme by scanning force microscopy. *J. Mol. Biol.*, **270**, 125–138.
- Weiss, D.J., Batut, J., Klose, K.E., Keener, J. and Kustu, S. (1991) The phosphorylated form of the enhancer-binding protein NTRC has an ATPase activity that is essential for activation of transcription. *Cell*, **67**, 155–167.
- Su, W., Porter, S., Kustu, S. and Echols, H. (1990) DNA-looping and enhancer activity: association between DNA-bound NtrC activator and RNA polymerase at the bacterial *glnA* promoter. *Proc. Natl Acad. Sci. USA*, **87**, 5504–5508.
- Wedel, A. and Kustu, S. (1995) The bacterial enhancer-binding protein NtrC is a molecular machine: ATP hydrolysis is coupled to transcriptional activation. *Genes Dev.*, **9**, 2042–2052.
- Casaz, P. and Buck, M. (1999) Region I modifies DNA-binding domain conformation of σ^N within the holoenzyme. *J. Mol. Biol.*, **285**, 507–514.
- Guo, Y., Wang, L. and Gralla, J.D. (1999) A fork junction DNA–protein switch that controls promoter melting by the enhancer-dependent sigma factor. *EMBO J.*, **18**, 3736–3745.
- Barrios, H., Valderrama, B. and Morett, E. (1999) Compilation and analysis of σ^{54} -dependent promoter sequences. *Nucleic Acids Res.*, **15**, 4305–4313.
- Gallegos, M.T., Cannon, W. and Buck, M. (1999) Functions of the σ^{54} Region I *in trans* and implications for transcription activation. *J. Biol. Chem.*, **274**, 25285–25290.
- Guo, Y. and Gralla, J.D. (1997) DNA binding determinants of σ^{54} as deduced from libraries of mutations. *J. Bacteriol.*, **179**, 1239–1245.
- Taylor, M., Butler, R., Chambers, S., Casimiro, M., Badii, F. and Merrick, M. (1996) The RpoN-box motif of the RNA polymerase sigma factor σ^N plays a role in promoter recognition. *Mol. Microbiol.*, **22**, 1045–1054.
- Cannon, W., Missailidis, S., Smith, C., Cottier, A., Austin, S., Moore, M. and Buck, M. (1995) Core RNA polymerase and promoter DNA interactions of purified domains of σ^N : bipartite functions. *J. Mol. Biol.*, **248**, 781–803.
- Merrick, M. and Chambers, S. (1992) The helix–turn–helix motif of σ^{54} is involved in recognition of the –13 promoter region. *J. Bacteriol.*, **174**, 7221–7226.
- Chaney, M., Pitt, M. and Buck, M. (2000) Sequences within the DNA-crosslinking patch of σ^{54} involved in promoter recognition, sigma isomerisation and open complex formation. *J. Biol. Chem.*, **275**, 22104–22113.
- Cannon, W., Gallegos, M.T., Casaz, P. and Buck, M. (1999) Amino-terminal sequences of σ^{54} (σ^N) inhibit RNA polymerase isomerisation. *Genes Dev.*, **13**, 357–370.
- Syed, A. and Gralla, J.D. (1998) Identification of an N-terminal region of σ^{54} required for enhancer-responsiveness. *J. Bacteriol.*, **180**, 5619–5625.
- Wigneshweraraj, S.R., Fujita, N., Ishihama, A. and Buck, M. (2000) Conservation of sigma-core RNA polymerase proximity relationships between the enhancer independent and enhancer dependent sigma classes. *EMBO J.*, **19**, 3038–3048.
- Casaz, P. and Buck, M. (1997) Probing the assembly of transcription initiation complexes through changes in σ^N protease sensitivity. *Proc. Natl Acad. Sci. USA*, **94**, 12145–12150.
- Casaz, P., Gallegos, M.T. and Buck, M. (1999) Systematic analysis of σ^{54} N-terminal sequences identifies regions involved in positive and negative regulation of transcription. *J. Mol. Biol.*, **292**, 229–239.
- Cannon, W., Chaney, M. and Buck, M. (1999) Characterisation of holoenzyme lacking σ^N regions I and II. *Nucleic Acids Res.*, **27**, 2478–2486.
- Wang, L. and Gralla, J.D. (1998) Multiple *in vivo* roles for the –12-region elements of σ^{54} promoters. *J. Bacteriol.*, **180**, 5626–5631.
- Wang, J.T. and Gralla, J.D. (1996) The transcription initiation pathway of σ^{54} mutants that bypass the enhancer protein requirement. Implications for the mechanism of activation. *J. Biol. Chem.*, **271**, 32707–32713.
- Wang, J.T., Syed, A., Hsieh, M. and Gralla, J.D. (1995) Converting *Escherichia coli* RNA polymerase into an enhancer-responsive enzyme: role of an NH₂-terminal leucine patch in σ^{54} . *Science*, **270**, 992–994.
- Gallegos, M.T. and Buck, M. (2000) Sequences in σ^{54} Region I required for binding to early melted DNA and their involvement in sigma-DNA isomerisation. *J. Mol. Biol.*, **297**, 849–859.
- Morris, L., Cannon, W., Clever-Martin, F., Austin, S. and Buck, M. (1994) DNA distortion and nucleation of local DNA unwinding within σ^{54} (σ^N) holoenzyme closed promoter complexes. *J. Biol. Chem.*, **269**, 11563–11571.
- Cannon, W., Gallegos, M.T. and Buck, M. (2000) Isomerisation of a binary sigma-promoter DNA complex by enhancer binding transcription activators. *Nature Struct. Biol.*, **7**, 594–601.
- Wigneshweraraj, S.R., Chaney, M.K., Ishihama, A. and Buck, M. (2001) Regulatory sequences in σ^{54} localise near the start of DNA melting. *J. Mol. Biol.*, in press.
- Gallegos, M.T. and Buck, M. (1999) Sequences in σ^{54} determining holoenzyme formation and properties. *J. Mol. Biol.*, **288**, 539–553.
- Jishage, M. and Ishihama, A. (1996) Regulation of RNA polymerase sigma subunit levels in *Escherichia coli*: intracellular levels of four species of sigma subunits under various growth conditions. *J. Bacteriol.*, **178**, 5447–5451.
- Jovanovic, G., Rakonjac, J. and Model, P. (1999) *In vivo* and *in vitro* activities of *Escherichia coli* σ^{54} transcription activator, PspF and its DNA-binding mutant PspDeltaHTH. *J. Mol. Biol.*, **285**, 469–483.
- Pavari, R., Pecht, I. and Soreq, H. (1983) A microfluorometric assay for cholinesterases, suitable for multiple kinetic determinations of picomoles of released thiocholine. *Anal. Biochem.*, **133**, 450–456.
- Claverie-Martin, F. and Magasanik, B. (1992) Positive and negative effects of DNA bending on activation of transcription from a distant site. *J. Mol. Biol.*, **227**, 996–1008.
- Claverie-Martin, F. and Magasanik, B. (1991) Role of integration host factor in the regulation of the *glnHp2* promoter of *Escherichia coli*. *Proc. Natl Acad. Sci. USA*, **88**, 1631–1635.
- Chaney, M.K. and Buck, M. (1999) The σ^{54} DNA-binding domain includes a determinant of enhancer responsiveness. *Mol. Microbiol.*, **33**, 1200–1209.
- Elliot, S. and Geiduschek, E.P. (1984) Defining a bacteriophage T4 late promoter: absence of a –35 region. *Cell*, **36**, 211–219.
- Popham, D.L., Szeto, D., Keener, J. and Kustu, S. (1989) Function of a bacterial activator protein that binds to transcriptional enhancers. *Science*, **243**, 629–635.
- Morett, E. and Buck, M. (1989) *In vivo* studies on the interaction of RNA polymerase σ^{54} with the *Klebsiella pneumoniae* and *Rhizobium meliloti* *nifH* promoters. *J. Mol. Biol.*, **210**, 65–77.
- Sasse-Dwight, S. and Gralla, J.D. (1988) Probing the *E. coli* *gln* ALG upstream activation mechanism *in vivo*. *Proc. Natl Acad. Sci. USA*, **85**, 8934–8938.
- Oguiza, J.A., Gallegos, M.T., Chaney, M.K., Cannon, W. and Buck, M. (1999) Involvement of σ^N DNA-binding domain in open complex formation. *Mol. Microbiol.*, **33**, 873–885.
- Ishihama, A. (2000) Molecular anatomy of RNA polymerase using protein-conjugated metal probes with nuclease and protease activities. *Chem. Commun.*, **13**, 1091–1094.
- Wang, L., Guo, Y. and Gralla, J.D. (1999) Regulation of σ^{54} -dependent transcription by core promoter sequences: role of –12 region nucleotides. *J. Bacteriol.*, **181**, 7558–7565.
- Oguiza, J.A. and Buck, M. (1997) DNA binding domain mutants of sigma-N (σ^N , σ^{54}) defective between closed and stable open promoter complex formation. *Mol. Microbiol.*, **26**, 655–64.
- Gross, C.A., Chan, C., Drombroski, A., Gruber, T., Sharp, M., Tupy, J. and Young, B. (1998) Mechanism of transcription. *Cold Spring Harbor Symp. Quant. Biol.*, **63**, 141–155.
- Fenton, M.S., Lee, S.J. and Gralla, J.D. (2000) *E. coli* promoter opening and –10 recognition: mutational analysis of sigma 70. *EMBO J.*, **19**, 1130–1137.